Global Biogeochemical Cycles®

RESEARCH ARTICLE
10.1029/2021GB007056

Iron Exports From Catchments Are Constrained by Redox Status and Topography

Jörg Tittel[1], Olaf Büttner[1], Kurt Friese[1], Oliver J. Lechtenfeld[1], Stephan Schuth[2], Wolf von Tümpling[1], and Andreas Musolff[1]

[1]UFZ – Helmholtz-Centre for Environmental Research, Leipzig, Germany, [2]Institute of Mineralogy, Leibniz University Hannover, Hannover, Germany

Key Points:

- Organic topsoils leach substantial amounts of Fe when incubated in the absence of NO_3, a competing electron acceptor that inhibits Fe reduction
- Shallow catchments with fluvially coupled topsoils and low NO_3 availability release 200 fold more Fe than steep ones with high NO_3 abundance
- Catchment topography and NO_3 availability explain 62%–64% of the variability of Fe concentration and OC:Fe and P:Fe ratios across 88 streams

Supporting Information:

Supporting Information may be found in the online version of this article.

Correspondence to:

J. Tittel,
joerg.tittel@ufz.de

Citation:

Tittel, J., Büttner, O., Friese, K., Lechtenfeld, O. J., Schuth, S., von Tümpling, W., & Musolff, A. (2022). Iron exports from catchments are constrained by redox status and topography. *Global Biogeochemical Cycles*, *36*, e2021GB007056. https://doi.org/10.1029/2021GB007056

Received 27 APR 2021
Accepted 21 DEC 2021

Abstract Fe(III) hydroxides stabilize organic carbon (OC) and P in soils. Observations of rising stream Fe concentrations are controversially posited to result from a flushing of iron-rich deeper soil layers or a decrease of competing electron acceptors inhibiting Fe reduction (NO_3^- and SO_4^{2-}). Here, we argue that catchment topography constrains the release of Fe, OC, and P to streams. We therefore incubated organic topsoil and mineral subsoil and modified the availability of NO_3^-. We found that Fe leaching was highest in topsoil. Fe, OC, and P released at quantities proportional to their ratios in the source soil. Supply of NO_3^- reduced Fe leaching to 18% and increased pore water OC:Fe and P:Fe ratios. Subsoil, however, was an insignificant Fe source (<0.5%). Here, the leached quantities of Fe, OC and P were highly disproportionate to the soil source with an excess of released OC and P. We tested if experimental findings scale up using data from 88 German catchments representing gradients in NO_3^- concentration and topography. Average stream Fe concentrations increased with decreasing NO_3^- and were high in catchments with shallow topography where high groundwater levels support reductive processes and topsoils are hydrologically connected to streams; but Fe concentrations were low in catchments with steep topography where flow occurs primarily through subsoils. OC:Fe and P:Fe ratios in the streams similarly varied by NO_3^- and topography. This corroborates the findings from the laboratory experiment and suggests that catchment topography and competing electron acceptors constrain the formation of Fe-reducing conditions and control the release of Fe, OC, and P to streams.

Plain Language Summary Iron is the second most abundant metal in the crust; its cycle is tightly connected to those of carbon, oxygen, and sulfur. The oxidized form (FeIII) is almost insoluble, but Fe can be mobilized by complexation or microbial Fe reduction. Both processes depend on availability of organic C. We found that Fe concentrations in streams were constrained by the topography of catchments and NO_3^- abundance. Shallower catchments are characterized by higher groundwater tables connecting the organic topsoils efficiently to streams. NO_3^- suppresses Fe reduction as a competing electron acceptor to Fe. We conclude that trends in soil wetness or atmospheric N deposition can change the stability of Fe and thus the release of PO_4^{3-} and harmful metals to surface waters.

1. Introduction

Iron is the fourth most abundant element on earth and the second most abundant metal in the crust. The Fe(II)/(III) redox couple is tightly connected to the cycles of other elements of geochemical interest: in particular C, O, N, and S (Melton et al., 2014). The interaction of Fe with these elements has evolved through geological time and defined ocean and atmospheric chemistry (Raiswell & Canfield, 2012). In soils and aquatic sediments, the stability of Fe is closely related to the presence of organic carbon (OC; Lalonde et al., 2012). As an electron donor, OC facilitates the microbial dissimilatory Fe reduction leading to the dissolution of soil Fe(III) (oxy)hydroxides and possibly to the release of Fe(II) ions. Moreover, OC prevents the oxidation and subsequent immobilization of ferrous Fe in Fe(II) organo-complexes (Fuss et al., 2011) and can also mobilize Fe non-reductively via leaching of Fe(III) complexes (Neal et al., 2008). Furthermore, OC inhibits the diagenetic transformation of poorly ordered Fe hydroxides such as ferrihydrite to more crystalline and more stable Fe minerals like goethite (Adhikari et al., 2017). Deeper insights into the geochemical interactions between Fe and OC have recently improved our process understanding of Fe reduction and Fe mineral formation (Pan et al., 2016; Zhao et al., 2017). However, it remains a challenge to transfer this knowledge to the catchment scale.

Fe concentrations in surface waters throughout Europe have been observed to increase over time since the late 1980s and early 1990s. Positive trends were reported from the UK, Sweden, Finland, and Germany, typically coinciding with positive trends in OC (Musolff, Selle, Büttner, Opitz, & Tittel, 2017; Neal et al., 2008; Sarkkola et al., 2013; Wällstedt et al., 2010). At present, Fe concentrations have already increased in 28% of streams and lakes in European and to a lesser extent also in North American water bodies (Björnerås et al., 2017). This poses the risk that, together with Fe, formerly adsorbed compounds such as OC, PO_4^{3-}, or harmful elements (As and Pb) will be remobilized and delivered to aquifers or surface waters. Two major lines of arguments explaining the upward trends are considered. First, more intense flushing of catchment soils induced by an increase in precipitation caused positive Fe trends (Björnerås et al., 2017). Deep mineral soil layers were the assumed sources as they are rich in Fe as well as in Si, which exhibited similar trends as Fe in surface waters (Björnerås et al., 2017; Weyhenmeyer et al., 2014). However, other studies concluded that organic-rich riparian topsoils must be the source (Ekström et al., 2016; Lidman et al., 2017). Second, more reductive conditions had decreased the stability of Fe(III) hydroxides in soils (Ekström et al., 2016), possibly driven by decreasing availabilities of competing electron acceptors such as SO_4^{2-} (Björnerås et al., 2017) or NO_3^- (Musolff, Selle, Büttner, Opitz, & Tittel, 2017).

Here, we argue that the catchment topography predetermines an initial setting that constrains the amount of Fe, OC, and P released to the stream. More specifically, catchments with steep hillslopes and narrow riparian areas are typically characterized by a low groundwater table relative to the stream (Grabs et al., 2012). The topsoil remains hydrologically disconnected during most of the time and, therefore, the mineral subsoil is the principal source layer of stream water (Bishop et al., 2004; Grabs et al., 2012). In contrast, shallow catchments are typically characterized by a high groundwater table. Here, topsoils in the stream vicinity largely generate discharge with rainfall events as their high lateral hydraulic conductivities facilitate a more efficient connection to the stream than in deeper layers (Bishop et al., 2004). Hence, organic surface soils are hydrologically activated and become the dominant sources of stream solutes (Seibert et al., 2009).

In our hypothesis, we refer to the two introduced lines of arguments addressing the upward Fe trends. We hypothesize that strongest Fe exports originate (a) from topsoils of shallow catchments owing to their high OC contents and their efficient hydrological connection to the stream if (b) they are located in areas with low abundance of competing electron acceptors. We incubated organic surface soil (topsoil) and mineral subsoil in order to simulate the leaching under conditions of high groundwater tables frequently occurring in shallow catchments and of low groundwater tables typical for steeper catchments, respectively. We modified the availability of competing electron acceptors by NO_3^- supply. On the basis of the experimental results, we derived a conceptual framework of Fe export and OC quality in catchments with different topography and redox conditions defined by abundance of NO_3^-. Finally, we tested the predictions with an evaluation of observed stream water chemistry from a large variety of catchments and elucidated the drivers of Fe concentration trends.

2. Methods

2.1. Soil Samples

Soil samples were taken in November 2017 at mid altitudes (425–470 m) of the Harz Mountains, Germany. The sampling point Z2 was located 2 m away from a first order stream in a steep catchment forested by spruce (51.85312°N and 10.61322°E). The soil represents a cambisol (World Reference Base for Soil Resources—WRB) with a humus-rich topsoil layer (Ah horizon, 0–8 cm) overlaying a brown coarse silt-loam horizon (Br) extending to ∼40 cm depth. The soil was collected in five depth intervals (0–8, 8–20, 20–29, 29–32, and 32–41 cm) using a Pürckhauer soil boring rod and transported in zipper plastic bags. Two additional soil profiles were obtained in adjacent watersheds (Table S1 in Supporting Information S1).

After stones and bigger roots had been removed, the soil samples were air-dried, sieved (2 mm mesh size) and pestled. To estimate the dry weight (DW), the samples were dried at 105°C overnight and stored in a desiccator. For total Fe quantification aliquots of 250 mg DW were digested with aqua regia (6 mL HCl 37%, 2 mL HNO_3 65%) in quartz microwave vessels and a pressure- and temperature-controlled microwave (CEM MARS 6). The Fe concentrations were measured by inductively coupled plasma optical emission spectrometry (ICP-OES, Optima 7300 DV, Perkin Elmer) according to DIN EN ISO 11885 (E22). Soil OC and N were quantified with a Vario EL (Elementar, Hanau, Germany) analyzer after acid treatment (30% HCl, Suprapur, Merck). Soil P was analyzed photometrically (Skalar, The Netherlands) after ignition (550°C, 2 hr) and digestion with hot HCl (DIN 38414).

The stable Fe isotope (δ^{57}Fe) analysis followed the methods of Schuth et al. (2015) using a Thermo-Finnigan (Bremen, Germany) Neptune multicollector inductively coupled plasma mass spectrometer. Details are described in the Supporting Information S1.

2.2. Experiment

For the leaching experiment, soil material was collected in September 2017 in a pit at station Z2 from the organic-rich topsoil layer (0–8 cm depth, Ah horizon) and from a mineral subsoil layer (8–20 cm depth, Br horizon). The catchment was characterized by steep slopes and low topographic wetness indices (TWI_{90} 7.6, see below), which we infer to indicate that mineral subsoils are the source of stream solutes during dry and moderately wet conditions (see Section 1). With respect to our experiment, we refer to the sample material as 'topsoil' and 'subsoil'. The soil was air dried and sieved (2 mm). Compared to the use of soil monoliths this procedure has the disadvantage that it perturbs the soil structure. However, larger inhomogeneities (e.g., bigger roots, worms, stones) could be removed. A quantity of 200 g of either topsoil or of subsoil was placed in each of triplicate throughflow vessels (flat flange beakers of 2 L volume equipped with flat ground flange lids with four ground joint necks, Schott, Figure S1 in Supporting Information S1). The soil was covered at the bottom and at the surface by pre-combusted (500°C, 4 hr) GF/A (Whatman) glass fiber filters, nylon mesh (100 µm) as well as 3 cm thick layers of acid-rinsed (0.1N HCl) and sonified gravel of ~5 mm size (Figure S1 in Supporting Information S1). Liquid medium was drained through the soil into sampling bottles at a rate of 1 L day^{-1} using peristaltic pumps (Minipuls 3, Gilson). The medium reservoirs, throughflow vessels and sampling bottles were continuously flushed with ultrahigh purity (UHP) nitrogen. The liquid medium resembled the ionic composition of pore water (KCl 0.084 mmol L^{-1}, $NaHCO_3$ 0.77 mmol L^{-1}, $CaCl_2$ 0.41 mmol L^{-1}, and $MgSO_4$ 1.25 mmol L^{-1}) assuming concentrations four times higher than measured in stream Z2 during routine monitoring. To test the release of Fe under non-Fe reducing and under Fe-reducing conditions, NO_3^- was supplied with the liquid medium (0.86 mmol L^{-1}) as a competing electron acceptor to Fe(III) from start until day 52. NO_3^- was not supplied on days 43–45 due to a technical incident. However, this did not affect the experiment as NO_3^- remained available in the soil pore water. The experiments were run for 127 days at a temperature of 20°C in the dark.

Samples for probe measurements (pH, redox) and chemical analyses of dissolved Fe, NO_3^-, dissolved organic carbon (DOC), and PO_4^{3-} (soluble reactive phosphorus, SRP) were taken two to six times per week from the medium that had accumulated in sampling bottles over the last 24 hr. The samples were filtered in a nitrogen atmosphere and by low vacuum (150 hPa) using 0.2 µm pore size polycarbonate membranes (Nuclepore, Whatman) except those for DOC, which were passed through pre-combusted glass fiber filters (GF/F, Whatman). The dissolved Fe and trace element samples were stabilized by HNO_3 (Suprapur, Merck, 65%; 200 µL/15 mL). To examine effects of dissolved organic matter (DOM) composition on Fe release, samples for DOM molecular composition and DOC radiocarbon (^{14}C-DOC) were derived at time points characterizing non-Fe reductive (day 52) and Fe-reductive conditions (day 68 in topsoil experiment, day 85 in subsoil experiment), respectively. Samples were passed through GF/F filters, acidified to pH 2.0 by HCl, bubbled for 2 hr by N_2 and stored at 4°C in the dark until extraction. Glassware was acid rinsed (1N HCl) and baked (500°C, 4 hr). We follow the standard protocol for DOM sample storage and extraction (cf., Dittmar et al., 2008; Raeke et al., 2016). We did not see any sign of precipitation and the average extraction efficiency in our sample set was within expected ranges (49 ± 14%). The details are described in the Supporting Information S1. The ^{14}C-DOC samples were evaporated and freeze-dried (Tittel et al., 2013). Furthermore, samples for dissolved Si and NH_4^+ analyses were filtered using 0.2 µm pore size membranes.

The pH was measured in sampling bottles by a SenTix 81 probe (WTW) and the redox potential was recorded by a BlueLine 31 rx platin electrode (Schott). Readings were corrected to a standard (220 mV) and referred to pH 7 and the normal hydrogen glass electrode (Mansfeldt et al., 2012). Concentrations of NO_3^-, SRP, and Si were measured photometrically using standard wet chemical protocols (ISO 15923-1:2013). Fe concentrations were measured by ICP-OES (Perkin Elmer 7300 DV) while trace elements were measured by ICP-MS (8800 Triple Quad, Agilent, Santa Clara, USA). DOC was quantified by near-IR absorption (Dimatoc 2000 analyzer, Analysentechnik Essen). DOM molecular composition was assessed via ultra-high resolution Fourier-transform ion cyclotron resonance mass spectrometry (FT-ICR MS) located at the ProVIS Centre for Chemical Microscopy within the Helmholtz Center for Environmental Research. Data evaluation was performed according to Lechtenfeld et al. (2014). For simplicity, only mean ± SD values (of sample triplicates) from intensity-weighted average

Table 1
Chemical and Fe Isotope Characterization of the Soil From Station Z2

Depth (cm)	Fe_t (mg g^{-1})	$\delta^{57}Fe$ (‰)	OC (mg g^{-1})	OC:Fe_t (mol mol^{-1})	P_t:Fe_t (mol mol^{-1})	OC:N (mol mol^{-1})
0–8	19.3	−0.15 ± 0.04	77.6	18.7	0.067	19
8–20	30.9	0.01 ± 0.02	15.4	2.3	0.021	12
20–29	29.8	−0.02 ± 0.03	17.8	2.8	0.031	12
29–32	34.8	0.16 ± 0.02	6.0	0.8	0.047	10
32–41	52.6	0.11 ± 0.03	2.4	0.2	0.021	7

Note. For the leaching experiment soil from 0 to 8 cm (topsoil) and 8 to 20 cm depth (subsoil) was used. Further vertical profiles of other catchments are given in Table S1 in Supporting Information S1. Fe_t, total iron; OC, organic carbon; P_t, total phosphorus; $\delta^{57}Fe$, mean ± 2SD of triplicate measurements.

molecular parameters are reported. The methods are described in the Supporting Information S1. Radiocarbon abundances were analyzed by accelerator mass spectrometry at the Poznan Radiocarbon Laboratory (Poland). The results ($\Delta^{14}C$) refer to the oxalic acid II standard and were corrected for process and instrument blanks and for fractionation (Stuiver & Polach, 1977).

2.3. Stream Data

We analyzed stream monitoring data from 88 catchments exhibiting a gradient in soil wetness defined by catchment topography. The streams supplied 28 drinking water reservoirs in Germany and were relatively unaffected by point sources. While their catchment sizes ranged between 0.2 and 303 km^2, 69% of catchments were ≤5 km^2, representing upstream conditions. The data were compiled as part of a larger data set (Musolff, Selle, Büttner, Opitz, & Tittel, 2017), which includes the area where the soil samples have been taken from (see above). We selected 88 streams from which dissolved Fe measurements were available. They were sampled for an average of 14 years at a frequency of 11 times per year. The locations and characteristics of the catchments as well as the methods of chemical analyses were described earlier (Musolff, Selle, Büttner, Opitz, & Tittel, 2017; Musolff et al., 2018). Samples were taken mainly on the basis of monthly routine monitoring programs conducted by the reservoir management authorities (Musolff, Selle, Büttner, Opitz, & Tittel, 2017). The UV attenuation was measured at 254 nm, corrected for Fe (Poulin et al., 2014) and related to DOC concentration to calculate the specific UV absorption (SUVA). Annual means of Fe, NO_3^-, and SRP concentrations as well as of SUVA were calculated after transforming the data to a normal-like distribution (Box & Cox, 1964). As a proxy of groundwater depth (Grabs et al., 2012; Ledesma et al., 2015) we calculated the topographic wetness index (TWI; Beven & Kirkby, 1979) based on 25 m digital elevation models (Musolff et al., 2018) as $\ln(a/\tan\beta)$, which relates the upslope area of each raster cell a to the local slope β. We used the 90th percentiles of the catchment TWI distributions (TWI_{90}) in our analyses. The TWI_{90} characterizes the wetness of the wettest parts of a catchment, that is, the near-stream (riparian) area, which is the main source of Fe and other solutes in streams (Inamdar & Mitchell, 2006; Raymond & Hopkinson, 2003). Details were described earlier (Musolff et al., 2018).

3. Results and Discussion

3.1. Soil Profile

High contents of OC in the topsoil layer decreased rapidly with depth (Table 1), while total Fe concentrations increased 2.7 fold with increasing distance from the soil surface. This changed the molar OC:Fe ratios from 19 at the surface to <3 below 8 cm depth. The enrichment of the stable isotope ^{57}Fe below 29 cm depth is consistent with the adsorption of Fe in deeper soil layers. Two other profiles from adjacent watersheds provided widely similar results (Table S1 in Supporting Information S1). Field observations reported in Mansfeldt et al. (2012) and Schuth and Mansfeldt (2016) confirmed that Fe was removed from the rising Fe-rich groundwater owing to adsorption onto crystalline Fe(III) oxides in the mineral subsoil. The heavy ^{57}Fe immobilizes preferentially at the mineral surfaces, even during reducing conditions in presence of a stable crystalline Fe oxide phase (Mansfeldt et al., 2012; Schuth & Mansfeldt, 2016; Schuth et al., 2015). The high Fe concentrations in the subsoil and the preferential immobilization of ^{57}Fe together found here, suggest that there is a stable and efficiently adsorbing Fe oxide phase in deeper soil layers.

3.2. Fe Mobilization in Soil Experiments

At the beginning of the experiment, high amounts of Fe were released from topsoil (Figure 1, Tables S2 and S3 in Supporting Information S1) that can be attributed to the perturbation of the soil before incubation (Pracht et al., 2018; see Section 2). It took 50 days until the release of Fe leveled at 9 µmol L^{-1} under NO_3^- supply. After NO_3^- supply was stopped, dissolved Fe rose and peaked at 48 µmol L^{-1} on day 68. Following that re-increase, the Fe concentrations gradually declined. The re-increase in Fe was associated with a decrease in standard redox potential from 22 to −54 mV. A subsequent batch experiment revealed that Fe(II) was the predominant form of

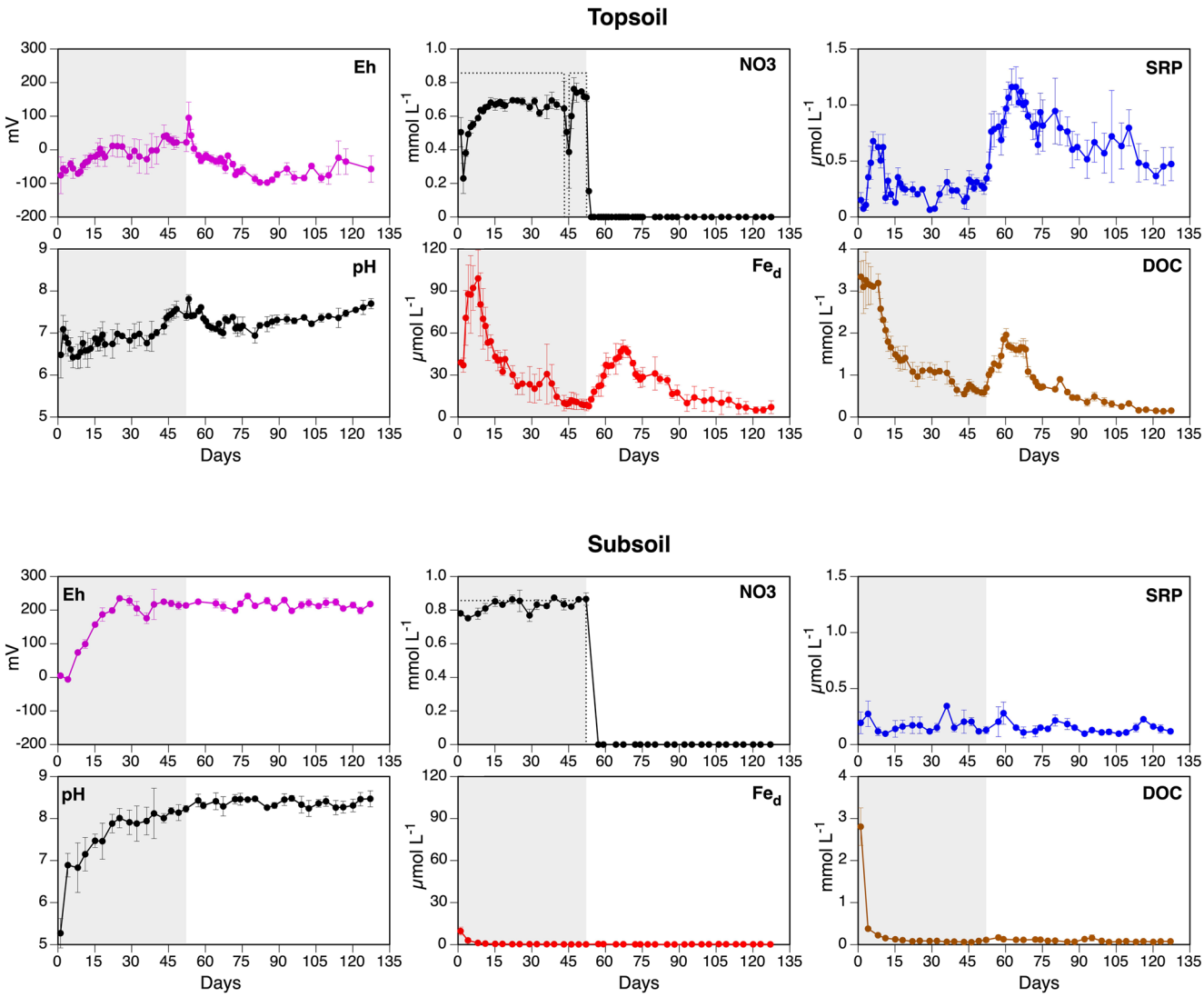

Figure 1. Concentration of Fe and other solutes leached over the course of the soil experiment. Symbols show means ± SD of triplicate experiments. The shaded areas characterize the first phase during which NO_3^- was supplied with the inflow medium. The dotted line shows the inflow NO_3^- concentration. SRP, soluble reactive phosphorus; DOC, dissolved organic carbon; Fe_d, dissolved iron.

leached Fe from the topsoil in absence of NO_3^-, exceeding the release of Fe(III) 2.2 fold (Figure S2 in Supporting Information S1). The supply of competing electron acceptors decreased the leaching of Fe(II) by a factor of 2.9. The concentrations of Fe(III) did not change so that both Fe(II) and Fe(III) were released in approximately equal amounts. In conclusion, higher Fe exports from topsoil in absence of NO_3^- were governed by Fe reduction. However, Fe reduction and nonreductive leaching via Fe(III) organo complexes occurred simultaneously in both presence and absence of NO_3^-. This may arise as an effect of spatially inhomogeneous redox conditions in microsites and of a surplus of suitable electron donors, that is, available DOC (Achtnich, 1995; Hall & Silver, 2015). It is likely that these results also characterize the processes in our throughflow experiment (Figure 1) in which the same soil was used and similar redox conditions prevailed. Thus, the measured exports are not the consequence of one specific process such as complexation or Fe reduction, but rather characterize the release from natural soils in the presence or absence of competing electron acceptors. In the following, we refer to $+NO_3^-$ or $-NO_3^-$ conditions, respectively. It should be noted that NO_3^- is not only an electron acceptor but can also be used as a N source by microorganisms. The change in NO_3^- supply could thus have influenced the activity of microorganisms and thus indirectly C release and P recycling. However, this effect was likely minor since NH_4^+, as another N source, was readily available in absence of NO_3^- in the topsoil pore water (33 ± 4 µmol L^{-1}) and

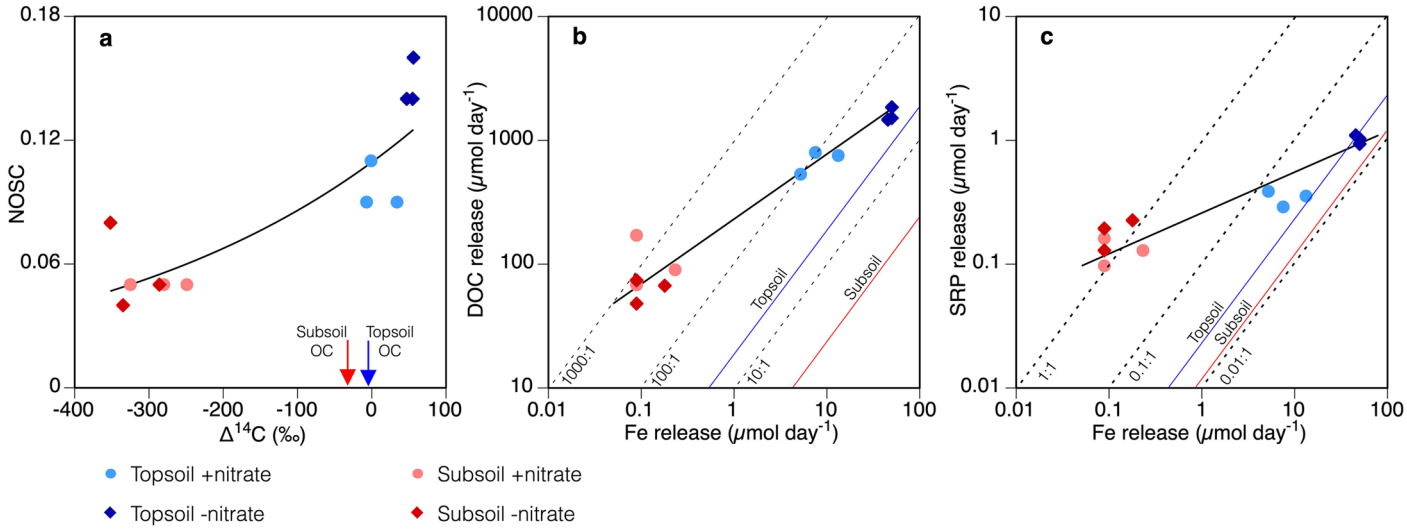

Figure 2. Leaching of organic carbon (OC) and P relative to Fe and changes in OC quality. Samples were from days 52 ($+NO_3^-$, topsoil and subsoil) as well from day 68 or 85 ($-NO_3^-$, topsoil and subsoil, respectively) of the throughflow soil experiment. (a) OC quality; NOSC, nominal oxidation state of carbon; three subsoil NOSC samples ($+NO_3^-$) were pooled due to low dissolved organic carbon (DOC) concentrations; regression $r^2 = 0.78$, $p = 0.0008$. (b) Fe and DOC release; the colored diagonal lines show the ratios in the soil. (c) Fe and soluble reactive phosphorus release.

NH_4^+ concentrations were not lower in the $-NO_3^-$ compared to the $+NO_3^-$ phase (28 ± 4 μmol L^{-1}, Table S2 in Supporting Information S1). Overall, the experiment corroborates the hypothesis that NO_3^- as a competing electron acceptor suppresses the release of dissolved Fe from soils under waterlogged conditions (Musolff, Selle, Büttner, Opitz, & Tittel, 2017).

Compared to topsoil, the release of Fe from mineral subsoil was low (0.2 ± 0.1 μmol L^{-1} after day 43) and did not change with the cut-off of NO_3^- supply (Figure 1). The difference in NO_3^- concentrations in the medium before and after the experiment reveal only a slight or no reduction of NO_3^- in the subsoil but a noticeable reduction of NO_3^- in topsoil. The standard redox potential rose in the subsoil during the first 3 weeks and remained at a high level between 176 and 242 mV in contrast to the topsoil experiment, even though both experiments were kept anaerobic. Thus, the subsoil did not facilitate the formation of reducing conditions, although potential electron acceptors were well available (NO_3^-). We interpret that as a deficiency of potent electron donors such as available DOC (high oxidation state and low ^{14}C age, see below). An exception was observed at the beginning of the subsoil experiment, when the redox potential was low at about 0 mV, which we attribute to the perturbation of the soil and the subsequent high availability of DOC. It may be argued that the rising pH during the subsoil experiment might have impaired the Fe reduction (Brookins, 1988; Grybos et al., 2009) and diminished the reductive release of Fe in the subsoil relative to the topsoil. However, a subsequent batch experiment run at lower pH (4.8–5.5) supported that only an insignificant amount of Fe was released from subsoil under these conditions (Figure S2 in Supporting Information S1). Earlier experiments testing the release of Fe from different horizons of a Gleysol obtained similar results: under reducing conditions soil from the surface organic Ah horizon released substantial amounts of Fe up to 3,570 μmol L^{-1}, whereas no significant release (~1 μmol L^{-1}) was observed from soil of the deeper CrBg horizon (Schuth et al., 2015).

The DOC leached from topsoil was primarily enriched in radiocarbon ($\Delta^{14}C > 0$) and therefore of modern origin. The $\Delta^{14}C$ values ranged between −7‰ and 56‰ characterizing C that was fixed during the last decades (Figure 2a, Table S2 in Supporting Information S1). This DOC contained similar or slightly higher amounts of radiocarbon than the bulk OC of the topsoil from which it was released (−4‰). In contrast to topsoil, DOC released from subsoil was significantly aged (~2,900 years B.P.). It was depleted in ^{14}C (−352‰ to −249‰) compared to bulk subsoil OC (200 years B.P., −31‰). Furthermore, the organic matter activated in topsoil under $-NO_3^-$ conditions was characterized by a high nominal oxidation state of carbon (NOSC; LaRowe & Van Cappellen, 2011), typical for oxidized compounds with high O/C and low H/C ratios (Figure 2a, Table S2 in Supporting Information S1). Under $+NO_3^-$ conditions the NOSC was slightly lower and reached the lowest values in subsoil. Low NOSC values as measured in subsoil reflect higher abundances of reduced compounds like fatty

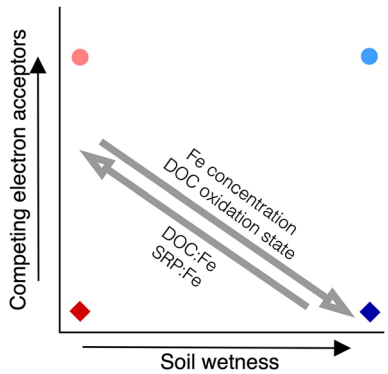

Figure 3. Conceptual framework predicting changes in catchment solute export between gradients of soil wetness and competing electron acceptor abundance. The symbols explain which catchment conditions the chosen experimental treatments represent (Figure 2), that is, topsoil and subsoil treatments characterize wet and dry conditions and $-NO_3^-$ and $+NO_3^-$ treatments represent low and high abundances of competing electron acceptors, respectively.

acids, sterols, and waxes. The oxidation state of the released organic matter can act as a feedback on the stability of the soil Fe(III) hydroxides. Under anaerobic conditions, when Fe is the terminal electron acceptor, the microbial oxidation of organic matter with low NOSC is thermodynamically inhibited (Keiluweit et al., 2016; LaRowe & Van Cappellen, 2011). Moreover, the age of the subsoil DOC between 2,200 and 3,400 years B.P. suggest that this organic matter was refractory and less available to microorganisms. Together with an overall lower abundance of DOC this may have supported the higher stability of Fe in subsoil (Figure 1).

In absence of NO_3^-, OC and Fe were dissolved in topsoil at quantities almost proportional to their ratio in the soil (Figure 2b). In contrast, in subsoil the leached quantities of OC and Fe were highly disproportionate to the soil source with an excess of released DOC (Figure 2b). This was associated with a disproportionate release of ^{14}C-depleted C ($-305‰$) relative to the bulk subsoil OC ($-31‰$, Figure 2a). This ^{14}C-depleted OC can only account for a small fraction of total OC in the subsoil given the large difference in isotopic composition between released and source OC. Possibly, this OC may have originated from even deeper and older layers and adsorbed in the subsoil horizon after capillary rise. We conclude that leaching processes in subsoil favored an immobilization of Fe and a disproportionate release of ^{14}C-old organic matter compared to the source soil.

The leaching of Fe from organic topsoil and mineral subsoil was consistent with the assumption that significant Fe losses are necessarily associated with high OC availability (Adhikari et al., 2017; Fuss et al., 2011; Neal et al., 2008). Both the total amount of OC and the amount of OC relative to Fe was high in topsoil (0–8 cm) but decreased rapidly in subsoil (8–20 cm, Table 1). The OC abundance and the soil OC:Fe ratio was similar in the next underlying layer (20–29 cm) and then continued to decrease until the end of the profile (41 cm). Therefore, we believe that by incubating soil from 0 to 8 cm and 8 to 20 cm depths, we were able to capture the most significant vertical change in Fe stability, which likely increased with further increasing sediment depth.

Phosphate ions compete efficiently for binding sites at metal hydroxides (Giesler et al., 2005). Compared to DOC, the overall release of SRP was lower by a factor of 10^3 (Figures 2b and 2c). However, SRP exhibited the same shift in its leaching behavior as DOC. In topsoil $-NO_3^-$ treatments, the ratio of SRP to dissolved Fe matched the P:Fe ratio in the soil. In subsoil, the release became strongly disproportionate relative to the soil P:Fe ratio with P released in excess.

3.3. Predictions for Catchment Solute Export

Next, we use the results from our experiment to derive a conceptual framework predicting the release of Fe in catchments representing gradients of wetness and of competing electron acceptor abundance (Figure 3). A high soil wetness (high groundwater table) connects the organic topsoil better and more often to the stream (Bishop et al., 2004) and facilitates reductive processes by waterlogging. We predict the highest Fe release and the most oxidized DOC for wet catchments having low abundances of competing electron acceptors. We also expect the lowest stream DOC:Fe and lowest SRP:Fe ratios in these catchments, although due to Fe precipitation in streams the values may not directly transferable to those of the experiment. The reverse is predicted in rather dry catchments with abundant competing electron acceptors. Here, mostly the mineral subsoil layer is hydrologically connected to the stream (see Section 1). In their topsoils, reductive conditions occur only rarely.

3.4. Stream Data

To test our hypotheses from the experiments (Figure 3) we analyzed the stream Fe concentrations from 88 catchments along a topographic gradient defining the wetness of the near-stream (riparian) soils (TWI_{90}, see Section 2). Soils with a higher TWI have lower topographic slopes and receive water from a larger upslope area (Beven & Kirkby, 1979). Also at catchment scale, mean topographic slopes and TWI_{90} are strongly negatively connected (Musolff et al., 2018). We utilized a data set where topographical and hydrochemical information

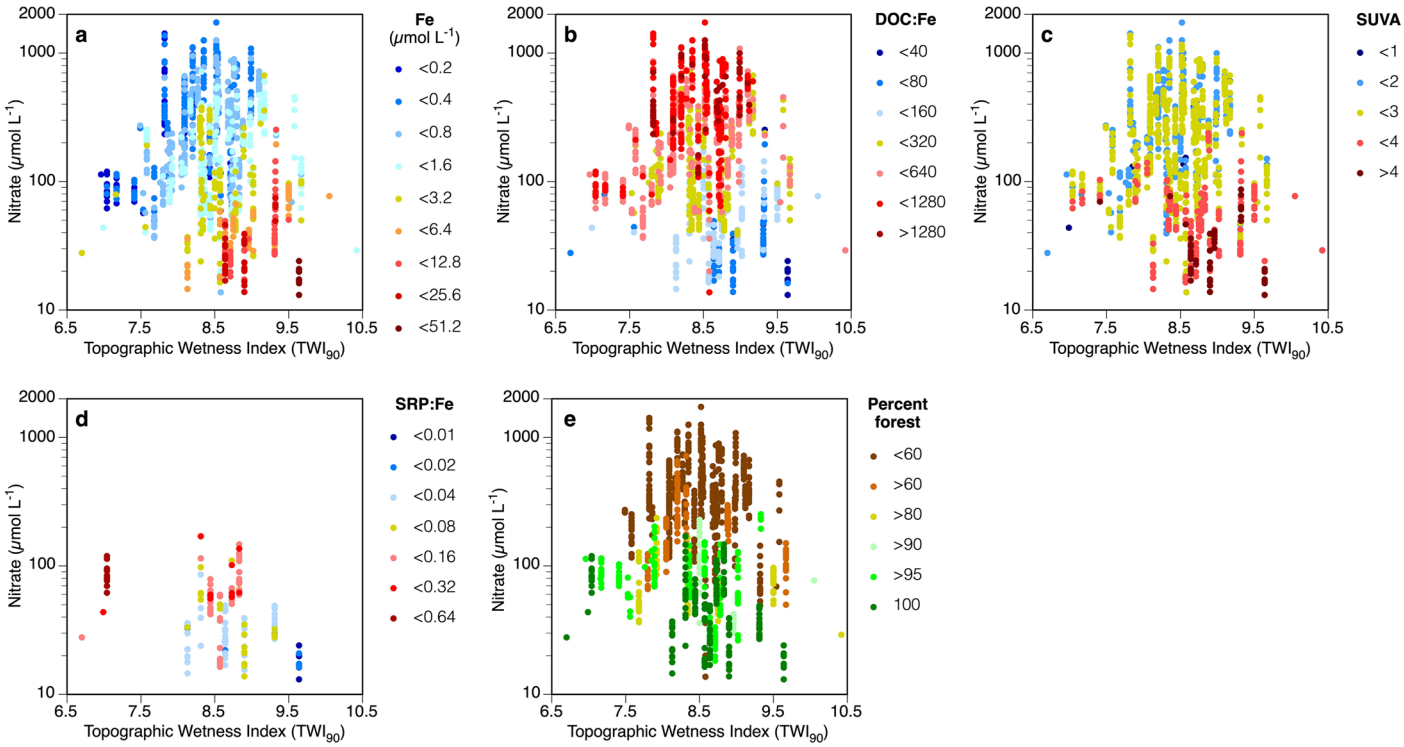

Figure 4. Fe, dissolved organic carbon (DOC), and soluble reactive phosphorus (SRP) in German streams depending on NO_3^- concentration and the topographic wetness index (TWI_{90}, see Section 2) of the catchments. (a) Fe concentration, (b) DOC:Fe (mol mol^{-1}), (c) specific UV absorption (SUVA), (d) SRP:Fe (mol mol^{-1}), and (e) land use. Symbols show annual means, in total of 1,211 observation years and 88 catchments, except (d) where only streams with entirely forested catchment areas were included ($n = 166$ annual means). Note logarithmic scales of NO_3^- and Fe concentration as well as of DOC:Fe and SRP:Fe ratios.

were jointly available. The annual mean values of dissolved Fe concentrations show a nonlinear increase with increasing TWI_{90} of the catchments (Figure 4a). There was also an increase of Fe with decreasing stream NO_3^- concentrations, as occurring in less agricultural catchments (Figure 4e). In a stepwise multiple regression model, (log_{10}) NO_3^- alone explains 41%, while NO_3^- and TWI_{90} together explain 64% of the variance of (log_2) Fe concentrations ($r^2 = 0.64$, $p < 0.0001$, Table S4 in Supporting Information S1). We conclude that the redox status and the topography of the catchment constrained Fe exports. This consistent pattern of Fe release appears surprising in view of the data set's diversity in geological parent materials, land use and hydroclimatic conditions. We believe that one reason for the consistent behavior is that the mobilization and transport of stream solutes is controlled by conditions in the riparian areas (Ledesma et al., 2015; Lidman et al., 2017; Marx et al., 2017). Riparian areas among differing catchments share basic structural characteristics, that is, a low topographic elevation relative to the stream, a high groundwater table and an organic-rich soil surface supporting reductive cycles (Grabs et al., 2012; Ledesma et al., 2015). Therefore, we argue that the mechanisms of solute mobilization and transport can be transferred to many riparian soils (Burt, 2005) owing to their unique morphological characteristics (Musolff et al., 2018).

The annual mean Fe concentrations spanned 2.6 orders of magnitude (0.09–37.8 μmol L^{-1}) and the changes along the TWI_{90} and NO_3^- gradients were highly nonlinear. We attribute this to the extremely low solubility of Fe under oxic conditions as well as to positive feedbacks on Fe stabilization such as the formation of stable Fe minerals (Colombo et al., 2015) and the thermodynamic inhibition of Fe reduction by organic matter availability as demonstrated in the experiment and stated elsewhere (LaRowe & Van Cappellen, 2011). This nonlinearity can underline why it can be so difficult to find the causes for the widespread increase of Fe concentrations. Small changes in wetness or in competing electron acceptor abundance potentially induce large Fe trends.

The range of annual mean DOC:Fe ratios (38–1,912; 1%–99% quantil) was comparable to the range of DOC:Fe ratios in the experiment (32–1,913, Figure 2b). Streams characterized by low abundances of NO_3^- and by shallow topographies exhibited the lowest DOC:Fe ratios (Figure 4b, $r^2 = 0.62$, $p < 0.0001$). As a proxy for the oxidation

state of organic matter we use its specific UV absorption (SUVA). High values of SUVA characterize more oxidized as well as more aromatic compounds (Kellerman et al., 2018; Weishaar et al., 2003). In the streams, high SUVA values were related to low NO_3^- availability and high topographic wetness (Figure 4c, $r^2 = 0.47$, $p < 0.0001$).

Finally, the annual mean SRP:Fe ratios ranged between 0.008 and 0.52 (1%–99% quantil) and were somewhat lower than the ratios during our experiment (0.019–2.17, Figure 2c). We considered only catchments with 100% forest cover. This eliminated potential effects of waste water point sources but decreased the variability in NO_3^- and the amount of available data. As in the case of stream DOC:Fe quotients, we found the lowest SRP:Fe ratios in shallow catchments with low NO_3^- concentrations and vice versa (Figure 4d, $r^2 = 0.64$, $p < 0.0001$).

The stream Fe concentrations and SUVA increased while the DOC:Fe and SRP:Fe ratios decreased along gradients of NO_3^- abundance and TWI_{90}. Hence, the catchment data support our hypothesis and predictions outlined in Figure 3. We conclude that catchment topography and competing electron acceptors constrain both the formation of Fe-reducing conditions and fluvial coupling of topsoils, which then control the release of Fe, OC and P to streams.

3.5. Stability of Fe in Changing Hydroclimates

Following our experimental findings and evidence from stream data, changes in both catchment wetness and supply of competing electron acceptors can induce trends in stream Fe concentration. Most upward trends in Fe were observed in northern Europe (Björnerås et al., 2017). Here, the NO_3^- concentrations are typically below 15 µmol L^{-1}, that is, as low as or below the lowest concentrations measured in the German streams. This raises the question whether NO_3^- can compete with Fe as an electron acceptor in boreal catchments. SO_4^{2-} has a lower standard redox potential than NO_3^- and Fe, however, SO_4^{2-} possibly competes with Fe depending on availabilities (Stumm & Morgan, 1996). For soil wetness we consider trends of stream discharge to be a suitable indicator, as the water level in the soil and the amount of streamflow are tightly coupled (Bishop et al., 2004). An analysis of discharges from streams in northern Europe between 1961 and 2000 revealed that 17% of 151 monitored streams exhibited a significant positive temporal discharge trend, while no stream showed a negative trend (Wilson et al., 2010). This points to hydrology rather than atmospheric deposition as the possible cause of Fe trends in northern Europe and partly North America. In our German data set we find only a few (positive and negative) significant trends in wetness, but NO_3^- concentrations had decreased significantly in 69% of streams in particular with forested, non-agricultural catchments. The negative NO_3^- trends correspond in time to a decrease in atmospheric N depositions (Musolff, Selle, Büttner, Opitz, Knorr, et al., 2017) and reasonably explain observed upward Fe trends (Musolff, Selle, Büttner, Opitz, & Tittel, 2017).

The finding that the OC-rich topsoil acts as a significant source has implications for the stability of soil Fe in future climates. First, hydrological models concurrently predict large-scale but diverging changes of high flows, defined as streamflows exceeded by 10% or 5% of the time (Schneider et al., 2013; Thober et al., 2018; van Vliet et al., 2013). Future high flows increase in boreal and temperate zones but decrease in Mediterranean and partly in continental climates (Thober et al., 2018; van Vliet et al., 2013). The predicted increase of high flows in boreal areas suggests an activation of larger topsoil areas. During low flow, however, the topsoil remains uncoupled. A decrease of summer flows, as proposed by models (Schneider et al., 2013) has thus little consequences for Fe exports, as Fe concentrations typically increase exponentially with discharges (Musolff, Selle, Büttner, Opitz, & Tittel, 2017). Together, this results in substantial increases of stream Fe concentrations during high flows but only in low or insignificant changes during low flows.

Earlier studies assumed deeper layers (Weyhenmeyer et al., 2014) with low OC:Fe ratios (0.5 to 6–10; Kalbitz et al., 2017) as the source of Fe to streams. Our data suggest that the Fe-rich deeper soil layers are not a significant source. Positive temporal trends of Si and Fe in catchments (Björnerås et al., 2017) may be interpreted as a consequence of hydrological activation of subsoil layers. In our experiment, however, the release of Si was >4.9 times higher in the topsoil than in the subsoil (64 and <13 µmol L^{-1}, respectively; Table S2 in Supporting Information S1). These observations are consistent with the predominant release of Si bound to organic matter, which was more abundant in the topsoil (Table 1). Studies showed that most of the Si released to stream water has passed through the biogenic Si pool, that is, it was previously taken up from soil solution by plants such as trees, grass and wetland, and recycled to the soil surface from falling litter (Derry et al., 2005). Thus, high Si concentrations

in streams and significant Fe exports from the topsoil are not necessarily contradictory. Furthermore, we assessed whether a mobilization of Fe-bound Si in soils can contribute to the upward trends of Si. Similar to OC, Si adsorbs to Fe hydroxides (Jones et al., 2009). In our experiment, however, we found no evidence for an Fe-related release of Si (Figure S3 in Supporting Information S1). The issue deserves further experimental work.

The reported increases in stream Fe concentration (Björnerås et al., 2017; Musolff, Selle, Büttner, Opitz, & Tittel, 2017; Neal et al., 2008) suggest widespread changes in soil biogeochemistry. Fe(III) hydroxides play a central role in the stabilization of organic matter (Lalonde et al., 2012; Riedel et al., 2013) as these mineral phases adsorb organic compounds with high capacity (Tipping, 1981), protecting them from microbial decomposition (Keiluweit et al., 2016). No less important, Fe(III) hydroxides immobilize metals (Benjamin & Leckie, 1981) and other elements that are problematic for the production of drinking water, such as As (Senn & Hemond, 2002) as well as P promoting algal growth (Baken et al., 2015; Giesler et al., 2005). Hence, together with Fe, more OC (Björnerås et al., 2017; Musolff, Selle, Büttner, Opitz, & Tittel, 2017), PO_4^{3-} (Baken et al., 2015), and metals (Wällstedt et al., 2017) can be delivered to stream-lake networks. Higher OC concentrations cause a browning of the water and increase the costs for drinking water production. Higher P supplies, as found in a number of forested German catchments (Musolff, Selle, Büttner, Opitz, & Tittel, 2017), increase the risk of eutrophication. Trace metals (Cu, Cr, Co, Ni, Pb, and V) and As also released more efficiently from topsoil (Table S2 in Supporting Information S1), explainable by sorption to and mobilization with Fe and soil OC (Gustafsson et al., 2011; Masscheleyn et al., 1991) as well as by redox changes (Hermann & Neumann-Mahlkau, 1985). Our study emphasizes concerns that atmospherically deposited trace metals will become more mobile in the future (Wällstedt et al., 2017), thus posing a threat to downstream water resources.

Data Availability Statement

The data that support the findings of this study are provided as Supporting Information S1. The field data are available in the repository HydroShare, https://doi.org/10.4211/hs.43601618877945c5a46b715aa98db729.

Acknowledgments
The authors would like to thank Yvonne Rosenlöcher for running the laboratory experiment and Michael Herzog, Andrea Hoff, Ina Siebert, and Dorothee Ohlwein for chemical analyses. Ralf Gründling helped with soil description. The authors also thank the staff at the Poznan Radiocarbon Laboratory for ^{14}C analyses. The authors acknowledge Jan Kaelser for FT-ICR MS measurements and the possibility to use the analytical facilities at the Centre for Chemical Microscopy (ProVIS) supported by EFRE-Europe funds Saxony. Comments of four reviewers greatly helped to improve the manuscript. Open access funding enabled and organized by Projekt DEAL.

References

Achtnich, C. (1995). Competition for electron donors among nitrate reducers, ferric iron reducers, sulfate reducers, and methanogens in anoxic paddy soil. *Biology and Fertility of Soils*, *19*(1), 65–72. https://doi.org/10.1007/bf00336349

Adhikari, D., Zhao, Q., Das, K., Mejia, J., Huang, R., Wang, X., et al. (2017). Dynamics of ferrihydrite-bound organic carbon during microbial Fe reduction. *Geochimica et Cosmochimica Acta*, *212*, 221–233. https://doi.org/10.1016/j.gca.2017.06.017

Baken, S., Verbeeck, M., Verheyen, D., Diels, J., & Smolders, E. (2015). Phosphorus losses from agricultural land to natural waters are reduced by immobilization in iron-rich sediments of drainage ditches. *Water Research*, *71*, 160–170. https://doi.org/10.1016/j.watres.2015.01.008

Benjamin, M. M., & Leckie, J. O. (1981). Multiple-site adsorption of Cd, Cu, Zn, and Pb on amorphous iron oxyhydroxide. *Journal of Colloid and Interface Science*, *79*(1), 209–221. https://doi.org/10.1016/0021-9797(81)90063-1

Beven, K. J., & Kirkby, M. J. (1979). A physically based, variable contributing area model of basin hydrology/Un modèle à base physique de zone d'appel variable de l'hydrologie du bassin versant. *Hydrological Sciences Bulletin*, *24*(1), 43–69. https://doi.org/10.1080/02626667909491834

Bishop, K., Seibert, J., Köhler, S., & Laudon, H. (2004). Resolving the double paradox of rapidly mobilized old water with highly variable responses in runoff chemistry. *Hydrological Processes*, *18*(1), 185–189. https://doi.org/10.1002/hyp.5209

Björnerås, C., Weyhenmeyer, G. A., Evans, C. D., Gessner, M. O., Grossart, H. P., Kangur, K., et al. (2017). Widespread increases in iron concentration in European and North American freshwaters. *Global Biogeochemical Cycles*, *31*(10), 1488–1500. https://doi.org/10.1002/2017GB005749

Box, G. E. P., & Cox, D. R. (1964). An analysis of transformations. *Journal of the Royal Statistical Society: Series B*, *26*(2), 211–243. https://doi.org/10.1111/j.2517-6161.1964.tb00553.x

Brookins, D. G. (1988). *Eh-pH diagrams for geochemistry* (p. 184). Springer.

Burt, T. P. (2005). A third paradox in catchment hydrology and biogeochemistry: Decoupling in the riparian zone. *Hydrological Processes*, *19*(10), 2087–2089. https://doi.org/10.1002/hyp.5904

Colombo, C., Palumbo, G., Sellitto, V. M., Cho, H. G., Amalfitano, C., & Adamo, P. (2015). Stability of coprecipitated natural humic acid and ferrous iron under oxidative conditions. *Journal of Geochemical Exploration*, *151*, 50–56. https://doi.org/10.1016/j.gexplo.2015.01.003

Derry, L. A., Kurtz, A. C., Ziegler, K., & Chadwick, O. A. (2005). Biological control of terrestrial silica cycling and export fluxes to watersheds. *Nature*, *433*(7027), 728–731. https://doi.org/10.1038/nature03299

Dittmar, T., Koch, B., Hertkorn, N., & Kattner, G. (2008). A simple and efficient method for the solid-phase extraction of dissolved organic matter (SPE-DOM) from seawater. *Limnology and Oceanography: Methods*, *6*(6), 230–235. https://doi.org/10.4319/lom.2008.6.230

Ekström, S. M., Regnell, O., Reader, H. E., Nilsson, P. A., Löfgren, S., & Kritzberg, E. S. (2016). Increasing concentrations of iron in surface waters as a consequence of reducing conditions in the catchment area. *Journal of Geophysical Research: Biogeosciences*, *121*(2), 479–493. https://doi.org/10.1002/2015JG003141

Fuss, C. B., Driscoll, C. T., Johnson, C. E., Petras, R. J., & Fahey, T. J. (2011). Dynamics of oxidized and reduced iron in a northern hardwood forest. *Biogeochemistry*, *104*(1), 103–119. https://doi.org/10.1007/s10533-010-9490-x

Giesler, R., Andersson, T., Lövgren, L., & Persson, P. (2005). Phosphate sorption in aluminum- and iron-rich humus soils. *Soil Science Society of America Journal*, *69*(1), 77–86. https://doi.org/10.2136/sssaj2005.0077a

Grabs, T., Bishop, K., Laudon, H., Lyon, S. W., & Seibert, J. (2012). Riparian zone hydrology and soil water total organic carbon (TOC): Implications for spatial variability and upscaling of lateral riparian TOC exports. *Biogeosciences*, *9*(10), 3901–3916. https://doi.org/10.5194/bg-9-3901-2012

Grybos, M., Davranche, M., Gruau, G., Petitjean, P., & Pédrot, M. (2009). Increasing pH drives organic matter solubilization from wetland soils under reducing conditions. *Geoderma*, *154*(1), 13–19. https://doi.org/10.1016/j.geoderma.2009.09.001

Gustafsson, J. P., Tiberg, C., Edkymish, A., & Kleja, D. B. (2011). Modelling lead(II) sorption to ferrihydrite and soil organic matter. *Environmental Chemistry*, *8*(5), 485–492. https://doi.org/10.1071/en11025

Hall, S. J., & Silver, W. L. (2015). Reducing conditions, reactive metals, and their interactions can explain spatial patterns of surface soil carbon in a humid tropical forest. *Biogeochemistry*, *125*(2), 149–165. https://doi.org/10.1007/s10533-015-0120-5

Hermann, R., & Neumann-Mahlkau, P. (1985). The mobility of zinc, cadmium, copper, lead, iron and arsenic in ground water as a function of redox potential and pH. *The Science of the Total Environment*, *43*(1), 1–12. https://doi.org/10.1016/0048-9697(85)90027-0

Inamdar, S. P., & Mitchell, M. J. (2006). Hydrologic and topographic controls on storm-event exports of dissolved organic carbon (DOC) and nitrate across catchment scales. *Water Resources Research*, *42*(3). https://doi.org/10.1029/2005wr004212

Jones, A. M., Collins, R. N., Rose, J., & Waite, T. D. (2009). The effect of silica and natural organic matter on the Fe(II)-catalysed transformation and reactivity of Fe(III) minerals. *Geochimica et Cosmochimica Acta*, *73*(15), 4409–4422. https://doi.org/10.1016/j.gca.2009.04.025

Kalbitz, K., Kaiser, K., & McDowell, W. H. (2017). Nitrate decline unlikely to have triggered release of dissolved organic carbon and phosphate to streams. *Global Change Biology*, *23*(7), 2535–2536. https://doi.org/10.1111/gcb.13659

Keiluweit, M., Nico, P. S., Kleber, M., & Fendorf, S. (2016). Are oxygen limitations under recognized regulators of organic carbon turnover in upland soils? *Biogeochemistry*, *127*(2), 157–171. https://doi.org/10.1007/s10533-015-0180-6

Kellerman, A. M., Guillemette, F., Podgorski, D. C., Aiken, G. R., Butler, K. D., & Spencer, R. G. M. (2018). Unifying concepts linking dissolved organic matter composition to persistence in aquatic ecosystems. *Environmental Science & Technology*, *52*(5), 2538–2548. https://doi.org/10.1021/acs.est.7b05513

Lalonde, K., Mucci, A., Ouellet, A., & Gelinas, Y. (2012). Preservation of organic matter in sediments promoted by iron. *Nature*, *483*(7388), 198–200. https://doi.org/10.1038/nature10855

LaRowe, D. E., & Van Cappellen, P. (2011). Degradation of natural organic matter: A thermodynamic analysis. *Geochimica et Cosmochimica Acta*, *75*(8), 2030–2042. https://doi.org/10.1016/j.gca.2011.01.020

Lechtenfeld, O. J., Kattner, G., Flerus, R., McCallister, S. L., Schmitt-Kopplin, P., & Koch, B. P. (2014). Molecular transformation and degradation of refractory dissolved organic matter in the Atlantic and Southern Ocean. *Geochimica et Cosmochimica Acta*, *126*, 321–337. https://doi.org/10.1016/j.gca.2013.11.009

Ledesma, J. L. J., Grabs, T., Bishop, K. H., Schiff, S. L., & Kohler, S. J. (2015). Potential for long-term transfer of dissolved organic carbon from riparian zones to streams in boreal catchments. *Global Change Biology*, *21*(8), 2963–2979. https://doi.org/10.1111/gcb.12872

Lidman, F., Boily, Å., Laudon, H., & Köhler, S. J. (2017). From soil water to surface water – How the riparian zone controls element transport from a boreal forest to a stream. *Biogeosciences*, *14*(12), 3001–3014. https://doi.org/10.5194/bg-14-3001-2017

Mansfeldt, T., Schuth, S., Hausler, W., Wagner, F. E., Kaufhold, S., & Overesch, M. (2012). Iron oxide mineralogy and stable iron isotope composition in a gleysol with petrogleyic properties. *Journal of Soils and Sediments*, *12*(1), 97–114. https://doi.org/10.1007/s11368-011-0402-z

Marx, A., Dusek, J., Jankovec, J., Sanda, M., Vogel, T., van Geldern, R., et al. (2017). A review of CO_2 and associated carbon dynamics in headwater streams: A global perspective. *Reviews of Geophysics*, *55*(2), 560–585. https://doi.org/10.1002/2016rg000547

Masscheleyn, P. H., Delaune, R. D., & Patrick, W. H. (1991). Effect of redox potential and pH on arsenic speciation and solubility in a contaminated soil. *Environmental Science & Technology*, *25*(8), 1414–1419. https://doi.org/10.1021/es00020a008

Melton, E. D., Swanner, E. D., Behrens, S., Schmidt, C., & Kappler, A. (2014). The interplay of microbially mediated and abiotic reactions in the biogeochemical Fe cycle. *Nature Reviews Microbiology*, *12*(12), 797–808. https://doi.org/10.1038/nrmicro3347

Musolff, A., Fleckenstein, J. H., Opitz, M., Büttner, O., Kumar, R., & Tittel, J. (2018). Spatio-temporal controls of dissolved organic carbon stream water concentrations. *Journal of Hydrology*, *566*, 205–215. https://doi.org/10.1016/j.jhydrol.2018.09.011

Musolff, A., Selle, B., Büttner, O., Opitz, M., Knorr, K.-H., Fleckenstein, J. H., et al. (2017). Does iron reduction control the release of dissolved organic carbon and phosphate at catchment scales? Need for a joint research effort. *Global Change Biology*, *23*(9), e5–e6. https://doi.org/10.1111/gcb.13758

Musolff, A., Selle, B., Büttner, O., Opitz, M., & Tittel, J. (2017). Unexpected release of phosphate and organic carbon to streams linked to declining nitrogen depositions. *Global Change Biology*, *23*(5), 1891–1901. https://doi.org/10.1111/gcb.13498

Neal, C., Lofts, S., Evans, C. D., Reynolds, B., Tipping, E., & Neal, M. (2008). Increasing iron concentrations in UK upland waters. *Aquatic Geochemistry*, *14*(3), 263–288. https://doi.org/10.1007/s10498-008-9036-1

Pan, W., Kan, J., Inamdar, S., Chen, C., & Sparks, D. (2016). Dissimilatory microbial iron reduction release DOC (dissolved organic carbon) from carbon-ferrihydrite association. *Soil Biology and Biochemistry*, *103*, 232–240. https://doi.org/10.1016/j.soilbio.2016.08.026

Poulin, B. A., Ryan, J. N., & Aiken, G. R. (2014). Effects of iron on optical properties of dissolved organic matter. *Environmental Science & Technology*, *48*(17), 10098–10106. https://doi.org/10.1021/es502670r

Pracht, L. E., Tfaily, M. M., Ardissono, R. J., & Neumann, R. B. (2018). Molecular characterization of organic matter mobilized from Bangladeshi aquifer sediment: Tracking carbon compositional change during microbial utilization. *Biogeosciences*, *15*(6), 1733–1747. https://doi.org/10.5194/bg-15-1733-2018

Raeke, J., Lechtenfeld, O. J., Wagner, M., Herzsprung, P., & Reemtsma, T. (2016). Selectivity of solid phase extraction of freshwater dissolved organic matter and its effect on ultrahigh resolution mass spectra. *Environmental Science-Processes & Impacts*, *18*(7), 918–927. https://doi.org/10.1039/c6em00200e

Raiswell, R., & Canfield, D. E. (2012). The iron biogeochemical cycle past and present. *Geochemical Perspectives*, *1*(1), 1–220. https://doi.org/10.7185/geochempersp.1.1

Raymond, P. A., & Hopkinson, C. S. (2003). Ecosystem modulation of dissolved carbon age in a temperate marsh-dominated estuary. *Ecosystems*, *6*(7), 694–705. https://doi.org/10.1007/s10021-002-0213-6

Riedel, T., Zak, D., Biester, H., & Dittmar, T. (2013). Iron traps terrestrially derived dissolved organic matter at redox interfaces. *Proceedings of the National Academy of Sciences of the United States of America*, *110*(25), 10101–10105. https://doi.org/10.1073/pnas.1221487110

Sarkkola, S., Nieminen, M., Koivusalo, H., Lauren, A., Kortelainen, P., Mattsson, T., et al. (2013). Iron concentrations are increasing in surface waters from forested headwater catchments in eastern Finland. *The Science of the Total Environment*, *463*, 683–689. https://doi.org/10.1016/j.scitotenv.2013.06.072

Schneider, C., Laize, C. L. R., Acreman, M. C., & Florke, M. (2013). How will climate change modify river flow regimes in Europe? *Hydrology and Earth System Sciences*, *17*(1), 325–339. https://doi.org/10.5194/hess-17-325-2013

Schuth, S., Hurrass, J., Munker, C., & Mansfeldt, T. (2015). Redox-dependent fractionation of iron isotopes in suspensions of a groundwater-influenced soil. *Chemical Geology*, *392*, 74–86. https://doi.org/10.1016/j.chemgeo.2014.11.007

Schuth, S., & Mansfeldt, T. (2016). Iron isotope composition of aqueous phases of a lowland environment. *Environmental Chemistry*, *13*(1), 89–101. https://doi.org/10.1071/en15073

Seibert, J., Grabs, T., Köhler, S., Laudon, H., Winterdahl, M., & Bishop, K. (2009). Linking soil- and stream-water chemistry based on a Riparian flow-concentration integration model. *Hydrology and Earth System Sciences*, *13*(12), 2287–2297. https://doi.org/10.5194/hess-13-2287-2009

Senn, D. B., & Hemond, H. F. (2002). Nitrate controls on iron and arsenic in an urban lake. *Science*, *296*(5577), 2373–2376. https://doi.org/10.1126/science.1072402

Stuiver, M., & Polach, H. A. (1977). Reporting of C-14 data – Discussion. *Radiocarbon*, *19*(3), 355–363. https://doi.org/10.1017/s0033822200003672

Stumm, W., & Morgan, J. J. (1996). *Aquatic chemistry, chemical equilibria and rates in natural waters*. John Wiley & Sons.

Thober, S., Kumar, R., Wanders, N., Marx, A., Pan, M., Rakovec, O., et al. (2018). Multi-model ensemble projections of European river floods and high flows at 1.5, 2, and 3 degrees global warming. *Environmental Research Letters*, *13*(1). https://doi.org/10.1088/1748-9326/aa9e35

Tipping, E. (1981). The adsorption of aquatic humic substances by iron-oxides. *Geochimica et Cosmochimica Acta*, *45*(2), 191–199. https://doi.org/10.1016/0016-7037(81)90162-9

Tittel, J., Büttner, O., Freier, K., Heiser, A., Sudbrack, R., & Ollesch, G. (2013). The age of terrestrial carbon export and rainfall intensity in a temperate river headwater system. *Biogeochemistry*, *115*(1), 53–63. https://doi.org/10.1007/s10533-013-9896-3

van Vliet, M. T. H., Franssen, W. H. P., Yearsley, J. R., Ludwig, F., Haddeland, I., Lettenmaier, D. P., & Kabat, P. (2013). Global river discharge and water temperature under climate change. *Global Environmental Change-Human and Policy Dimensions*, *23*(2), 450–464. https://doi.org/10.1016/j.gloenvcha.2012.11.002

Wällstedt, T., Björkvald, L., & Gustafsson, J. P. (2010). Increasing concentrations of arsenic and vanadium in (southern) Swedish streams. *Applied Geochemistry*, *25*(8), 1162–1175. https://doi.org/10.1016/j.apgeochem.2010.05.002

Wällstedt, T., Björkvald, L., Laudon, H., Borg, H., & Morth, C. M. (2017). Landscape control on the hydrogeochemistry of As, Co and Pb in a boreal stream network. *Geochimica et Cosmochimica Acta*, *211*, 194–213. https://doi.org/10.1016/j.gca.2016.08.030

Weishaar, J. L., Aiken, G. R., Bergamaschi, B. A., Fram, M. S., Fujii, R., & Mopper, K. (2003). Evaluation of specific ultraviolet absorbance as an indicator of the chemical composition and reactivity of dissolved organic carbon. *Environmental Science & Technology*, *37*(20), 4702–4708. https://doi.org/10.1021/es030360x

Weyhenmeyer, G. A., Prairie, Y. T., & Tranvik, L. J. (2014). Browning of boreal freshwaters coupled to carbon-iron interactions along the aquatic continuum. *PLoS One*, *9*(8), e88104. https://doi.org/10.1371/journal.pone.0088104

Wilson, D., Hisdal, H., & Lawrence, D. (2010). Has streamflow changed in the Nordic countries? – Recent trends and comparisons to hydrological projections. *Journal of Hydrology*, *394*(3–4), 334–346. https://doi.org/10.1016/j.jhydrol.2010.09.010

Zhao, Q., Adhikari, D., Huang, R., Patel, A., Wang, X., Tang, Y., et al. (2017). Coupled dynamics of iron and iron-bound organic carbon in forest soils during anaerobic reduction. *Chemical Geology*, *464*, 118–126. https://doi.org/10.1016/j.chemgeo.2016.12.014